Structure and dynamics of undercurrents in the western boundary current of the Bay of Bengal

Pavanathara Augustine Francis[1] · Abraham Kaduvathazham Jithin[1,2] · Abhisek Chatterjee[1] · Arnab Mukherjee[1] · Doraiswamy Shankar[3] · Puthenveettil Narayanamenon Vinayachandran[4] · Surireddi Satya Venkata Siva Ramakrishna[2]

Abstract

The structure and variability of undercurrents in the East India Coastal Current (EICC), which is the western boundary current system in the Bay of Bengal (BoB), and the mechanisms of their formation are examined in this study. We used current data collected by Acoustic Doppler current profilers (ADCP) moored off Cuddalore (~ 12°N), Kakinada (~ 16.5°N), Visakhapatnam (~ 17.7°N), and Gopalpur (~ 19.4°N) and simulations for the period 2013–2014 from a high-resolution model configured for the BoB. The undercurrents were observed at all these locations, mainly during summer (June–August) and winter (October–December). Undercurrents were seen at relatively shallow depths (75 m), and their occurrences were more frequent off Cuddalore, whereas they were deep (100–150 m) and less frequent in the northern part of the east coast (off Visakhapatnam and Gopalpur). Numerical simulations showed that the interaction of the westward propagating anticyclonic eddies with the equatorward EICC weakened the strong surface flow and reversed the weak subsurface flow in the northern part of the western BoB. This interaction resulted in the formation of the poleward undercurrent here. Once these mesoscale eddies dissipated due to the interaction with the continental slope, the poleward undercurrents vanished and equatorward flow in the subsurface reappeared. The observed undercurrents near the shelf break region (75–200 m) in the southern part of the coast (off Cuddalore) were associated with small subsurface eddies (diameter of about 20–30 km), which developed due to large zonal gradient in the alongshore component of EICC. Subsurface anticyclonic circulations of larger spatial extent (diameter > 200 km) were responsible for the observed undercurrents in the deeper levels (deeper than 250 m) off Cuddalore. We further show that intraseasonal variability of undercurrents near the shelf break off Cuddalore was directly linked to intraseasonal variability in the strength of surface EICC itself. Results from this study suggest that the undercurrents observed below the EICC were not continuous poleward flow, but they were part of distinct anticyclonic eddies.

Keywords East India Coastal Current · Western boundary currents · Undercurrents · Acoustic Doppler Current Profilers · Subsurface eddies

✉ Pavanathara Augustine Francis
 francis@incois.gov.in

[1] Indian National Centre for Ocean Information Services, Ministry of Earth Sciences, Government of India, Hyderabad 500090, India

[2] Department of Meteorology and Oceanography, Andhra University, Visakhapatnam 530003, India

[3] CSIR-National Institute of Oceanography, Dona Paula, Goa 403004, India

[4] CAOS, Indian Institute of Science, Bangalore 560012, India

1 Introduction

The East India Coastal Current (EICC) is the western boundary current system in the Bay of Bengal (BoB) with a characteristic reversal in the direction of flow north of 10°N (McCreary et al. 1993; Shankar et al. 1996; Mukherjee et al. 2014). As EICC is one of the important organized circulation features in the Indian Ocean (Shankar et al. 2002), it plays an important role in the basin-scale heat budget (Shenoi et al. 2002), distribution of salt (Han and McCreary 2001; Jensen 2001; Akhil et al. 2014), and biogeochemistry of the western BoB (Naqvi et al. 2006). Major driving forces of EICC are the winds blowing parallel to the coast all along the boundaries of the BoB, Ekman pumping in the interior BoB (Shetye et al. 1993) and remote forcing from the equatorial Indian Ocean

(Yu et al. 1991; McCreary et al. 1996; Shankar et al. 1996; Vinayachandran et al. 1996). Since there are more than one mechanism that forces the EICC (McCreary et al. 1993), the interplay between these forcings makes the spatial variation in the current system highly incoherent (McCreary et al. 1993; Shankar et al. 2002; Mukherjee et al. 2014). Mukherjee et al. (2017) showed that, while the annual near-surface EICC is mainly forced by the local alongshore winds and Ekman pumping in the interior BoB, intraseasonal variability in alongshore currents in the southern part of the east coast is mainly forced by local intraseasonal winds and that in the northern part is forced by intraseasonal winds in the equatorial Indian Ocean. A recent study by Mukherjee and Kalita (2019) showed that equatorial Indian Ocean plays an important role in the interannual variability of the surface EICC.

While there is a fairly good understanding on the variability as well as the forcing mechanisms of the surface EICC, studies on the subsurface structure of EICC are still scarce. This is primarily due to the nonavailability of data of currents at different vertical levels in the coastal waters for sufficiently long time. However, based on the limited hydrographic data, Shetye et al. (1991) reported the occurrences of feeble undercurrents below the strong surface flow off the east coast of India during the summer. These authors observed downwelling signals below ∼ 70 m on the continental slope, which indicate the presence of undercurrents. Based on numerical experiments using a linear model, McCreary et al. (1996) suggested that the observed undercurrents during the summer along the western boundary of the BoB could be due to remote equatorial forcing and Ekman pumping in the interior BoB. However, a detailed investigation on the structure and variability (both in time and space) of the entire EICC became possible only with the availability of continuous time series data from a series of Acoustic Doppler Current Profilers (ADCPs) deployed in the coastal waters around the country (Amol et al. 2014; Mukherjee et al. 2014). These ADCPs, deployed both on the shelf and slope regions off the east and west coasts of India, provided high-frequency (hourly) measurements of currents for the entire water column (except a few meters near the surface). Based on the investigation of the structure and variability of the EICC using data from these ADCPs, Mukherjee et al. (2014) reported that while the EICC in the northern part of the western BoB (off Gopalpur and Kakinada) extended to the deeper levels, it was shallow with frequent occurrences of undercurrents on the slope off Cuddalore. They also suggested that the observed undercurrents off Cuddalore might be associated with downward propagation of energy from the annual alongshore EICC.

Structure and variability of undercurrents in coastal circulations have been studied extensively in many parts of the global oceans. For example, the presence of coastal undercurrents was reported in the Somali current system in 1980's itself (Leetmaa

et al. 1982; Quadfasel and Schott 1983). Jensen (1991) had analyzed the simulations from a four-layer model to understand the possible reasons for the formation of undercurrents in the Somali current system and suggested that remote forcing acting through the equatorial waves and the Rossby waves generated along the west coast of India could be responsible for these undercurrents. McCreary et al. (1993) and Shankar et al. (2002) also showed the impact of Rossby waves from the west coast of India on the Somali current. Recently, based on ocean general circulation model simulations, Chatterjee et al. (2017) showed the existence of strong equatorward undercurrent below the remotely forced surface poleward current along the coast of Andaman and Nicobar Islands and eastern boundary of the Andaman Sea. Another prominent and well-studied undercurrent system in the coastal waters is the Peru-Chile Undercurrent, which flows poleward below the equatorward surface Peru coastal current system (Thomsen et al. 2016).

One of the major challenges that restricted detailed study of the structure and variability of the undercurrents in the east coast of India was the difficulty of the numerical models to simulate their observed features realistically. Mukherjee et al. (2014) showed that though many ocean models are able to capture the observed seasonal cycle in the circulation along the east coast, most of them have difficulty in simulating its intraseasonal variability. Interestingly, a comparison of the simulations by a very high-resolution (∼ 2.3 km) ocean general circulation model (Regional Ocean Modeling System, ROMS) configured for the BoB with the coastal ADCP observations suggested that the model was able to simulate the coastal circulation realistically (Jithin et al. 2017). We use these model simulations as well as the observations from ADCPs to study the space-time variability, structure, and dynamics of coastal undercurrents in this paper. Details of data and the numerical model used in this study are given in Section 2. Major findings of this study are given in Section 3, and the summary and discussions are given in Section 4.

2 Data and methods

2.1 Observations

Vertical profiles of daily-mean current data between 48 m and 700 m for the period 2013–2014, obtained from the ADCP moorings deployed at about 1000 m water depth along the continental slope (4 ADCPs) regions off the east coast of India (Fig. 1) for the period 2013–2014, were used to study the undercurrent features and for the validation of model simulated currents in the coastal regions. Vertical resolution of the slope ADCP data is 4 m in the upper levels and 8 m in the deeper levels. Details of ADCP moorings and data used in this study are provided in Table 1. Data near the surface and bottom levels were removed during the quality check due to
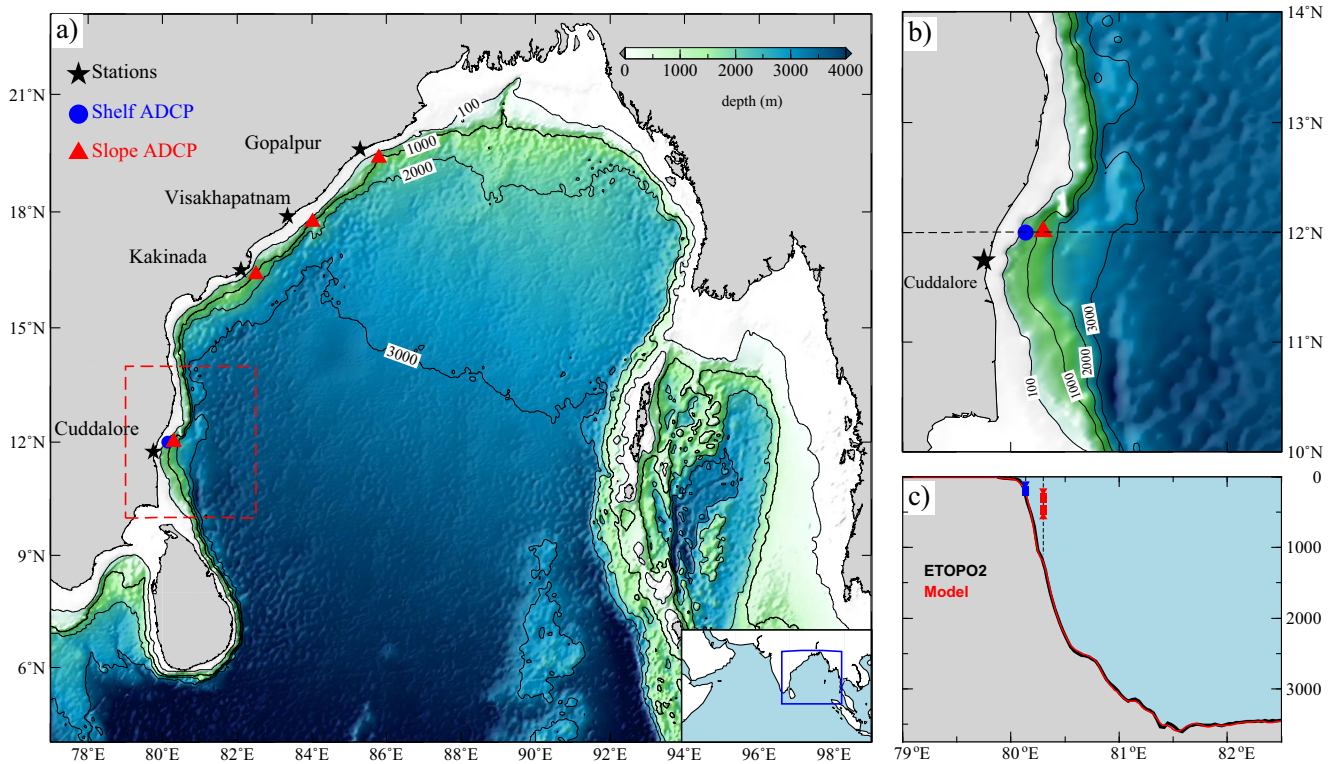
Fig. 1 (**a**) Model domain and locations of ADCP installations along the east coast of India. Inset map shows the north Indian Ocean and the model domain (blue box). Bathymetric contours of 100, 1000, 2000, and 3000 m are also shown. (**b**) Zoomed view of bathymetry off Cuddalore indicated by red dashed box. Dashed line shows the 12°N latitude. Names of the coastal cities (black star) near the ADCP mooring locations are used as ADCP station names. (**c**) Cross-shore bathymetry at 12°N from modified ETOPO2 data (Sindhu et al. 2007) and ROMS 1/48°. Schematic of upward and downward looking ADCP moorings on the shelf break (blue) and slope (red) also shown

contamination and echoes. Observed currents were rotated with respect to coastline angle to obtain the alongshore and cross-shore components. In addition to the ADCP data from the slope, current measurements from an ADCP deployed on the shelf off Cuddalore were also used to describe the features of undercurrent system at this location.

2.2 Model configuration

In the present study, we used daily-mean outputs from ROMS (version 3.7), configured for the BoB (Jithin et al. 2017). ROMS is a free-surface, terrain-following general circulation model which solves a set of primitive equations

Table 1 Details of ADCP moorings on the shelf and slope off the east coast of India used for the present study. Angle of rotation is the local bathymetric angle which is used to calculate the cross-shore and alongshore component. On the slope, ADCPs were moored at different depths for maximum vertical coverage. D (U) indicates downward (upward) looking ADCP

Mooring location	Mooring type	Lon/Lat (° E/° N)	ADCP depth (m)	Water depth (m)	Sampling interval time/vertical	Angle of rotation	Shelf width (km)	Period of observation	
								Start date	End date
Cuddalore	Shelf	80.135/12.010	180.5	190.5	15 min/4 m	−15.76°	40	21-02-2014	29-04-2014
	Slope	80.204/12.015	332	1088	60 min/4 m	−15.76°	40	01-01-2013	20-02-2014
		80.204/12.014	194 (708 U)	1129	60 min/4 (8) m	−15.76°	40	12–03–2013, 20-02-2014	
		80.204/12.006	182 (695 U)	1115	60 min/4 (8) m	−15.76°	40	21-02-2014	04-03-2015
Kakinada	Slope	82.609/16.452	354	1292	60 min/8 m	−55.07°	30	14-02-2012	15-03-2013
		82.181/16.05	318	1086	60 min/8 m	−55.07°	30	15-03-2013	23-02-2014
		82.205/16.105	246	904	60 min/8 m	−55.07°	30	23-02-2014	07-03-2015
Visakhapatnam	Slope	84.016/17.743	164 (190 D)	1040	60 min/8 m	−49.74°	56	01-01-2013	04-02-2014
		84.02/17.752	111(528 U)	941	60 min/4 (8)m	−49.74°	56	18-03-2013	24-02-2014
		84.058/17.75	165	1017	60 min/4 (8) m	−49.74°	56	25-02-2014	09-03-2015
Gopalpur	Slope	85.787/19.380	179(587 U)	1038	15 min/4 (8) m	−51.72°	55	20-03-2013	27-02-2014
		85.786/19.395	203(617 U)	1071	15 min/4 (8) m	−51.72°	55	27-02-2014	11-03-2015

in an orthogonal curvilinear coordinate system developed by Rutgers University, New Jersey, USA (Song and Haidvogel 1994; Haidvogel et al. 2000; Shchepetkin and McWilliams 2005). The spatial resolution of the model configuration is 1/48° (approximately 2.3 × 2.3 km), and there are 40 sigma levels in the vertical. Vertical stretching parameters are chosen in such a way that there are about 26 levels in the top 200 m of the water column, where the depth of the ocean is about 3000 m. The model domain covers the entire BoB and Andaman Sea, extending from 77°E to 99°E and 4°N to 23°N. Malacca Strait and Palk Strait are closed in the present model configuration. Open boundary conditions are applied in the southern and western boundaries of the model (Fig. 1a). In these open boundaries, tracer, momentum, and sea level anomaly fields are nudged to daily-mean simulations from ROMS model setup for the entire Indian Ocean basin with 1/12° resolution. The model uses the KPP mixing scheme (Large et al. 1994) to parameterize the vertical mixing. Harmonic mixing scheme is used for the horizontal mixing of momentum and tracers along the geopotential surfaces (Haidvogel and Beckmann 1999), and bulk parameterization scheme is used for the computation of air-sea fluxes of heat (Fairall et al. 1996). Atmospheric fields from Global Forecast System (GFS) at a horizontal resolution of 1/4°, obtained from National Centre for Medium Range Weather Forecast (http://www.ncmrwf.gov.in/t254-model/t254_des.pdf), are used for forcing both the high-resolution (1/48°) as well as the low-resolution (1/12°) ROMS setups. In addition, tidal forcing is introduced in the model with boundary conditions in the southern and western open boundaries extracted from TPXO7.0 model. Sea surface salinity of this model setup is relaxed to climatological values obtained from World Ocean Atlas (2009). In order to be consistent with the period of continuous data availability from the ADCPs, we restrict our analysis to the period January 2013 to December 2014. Detailed validation of the modeled tidal and subtidal circulation in the BoB can be seen in Jithin et al. (2017, 2019) (Table 2).

Table 2   : Details of ROMS model configuration for the BoB

Parameters	ROMS
Bathymetry	Modified ETOPO2*
Horizontal resolution	About 2.3 km (1/48°)
Vertical resolution	40 sigma levels (theta b = 7.2, theta s = 0.2)
Initial condition	Indian Ocean ROMS 1/12° setup**
Boundary condition	Indian Ocean ROMS 1/12° setup (daily-mean)**
Tidal forcing	10 tidal constituents from TPXO7.0
Atmospheric forcing	NCMRWF 6 hourly wind (1/4° resolution)
Salinity relaxation	Monthly climatology (WOA2009)

* Sindhu et al. (2007), ** Jithin et al. (2017)

3 Results

3.1 Observed variability of surface and subsurface EICC on the slope

Observed alongshore currents at 48 m and 152 m depths on the slope off Cuddalore, Kakinada, Visakhapatnam, and Gopalpur during the period January 2013 to December 2014 are shown in Fig. 2. Maximum magnitude (125 cm s^{-1}) of the alongshore currents was found near the central part of the coast (e.g., off Kakinada and Visakhapatnam). In general, alongshore currents at 48 m were poleward at all the locations of ADCP during spring (February–April). This is consistent with known direction of EICC reported in previous studies (Shetye et al. 1993; McCreary et al. 1993, 1996). Observations show that alongshore currents during spring exceeded 100 cm s^{-1} at all the locations. In general, the observed alongshore currents near the surface were equatorward during summer (June–August) at all the locations with relatively strong magnitude (100–125 cm s^{-1} at 48 m) off Gopalpur and Visakhapatnam (Figs. 2a and b). During winter (October–December), the observed currents were equatorward with their peak in November.

Even though the observed currents during 2013–2014 generally showed the known seasonality of EICC, noticeable variability occurred within the seasons and also across the years (2013 and 2014). For example, the surface EICC was equatorward with a maximum magnitude of about 100 cm s^{-1} during summer 2013, but its magnitude was relatively weak with episodes of poleward flow during summer 2014. Similar reversal in the direction of EICC was also seen on the slope off Kakinada. The differences in the direction and magnitudes of EICC in the same season across the years were also reported by Mukherjee et al. (2014). Mukherjee et al. (2017) and Sherin et al. (2018) showed that the magnitude of EICC can be modulated in the interannual time scales by El Niño and Southern Oscillation (ENSO) and Indian Ocean Dipole (IOD) events (Saji et al. 1999), which affect the remote forcing in the equatorial Indian Ocean. Based on the analysis of ADCP data for the period from May 2009 to March 2013, Mukherjee et al. (2014) reported strong interseasonal variability in the EICC off Kakinada and Gopalpur and relatively weak intraseasonal variability off Cuddalore. It may be seen from Fig. 2 that the ADCP observations for the period of 2013–2014 also indicated relatively strong intraseasonal variability off Gopalpur and Kakinada. In addition, the intraseasonal variability off Visakhapatnam was also comparable to that off Gopalpur and Kakinada (figure not shown). Since the present paper mainly focuses on the undercurrents and their variability, detailed analysis on intraseasonal and interannual variability of surface EICC is beyond the scope of this paper. Readers may refer Mukherjee et al.
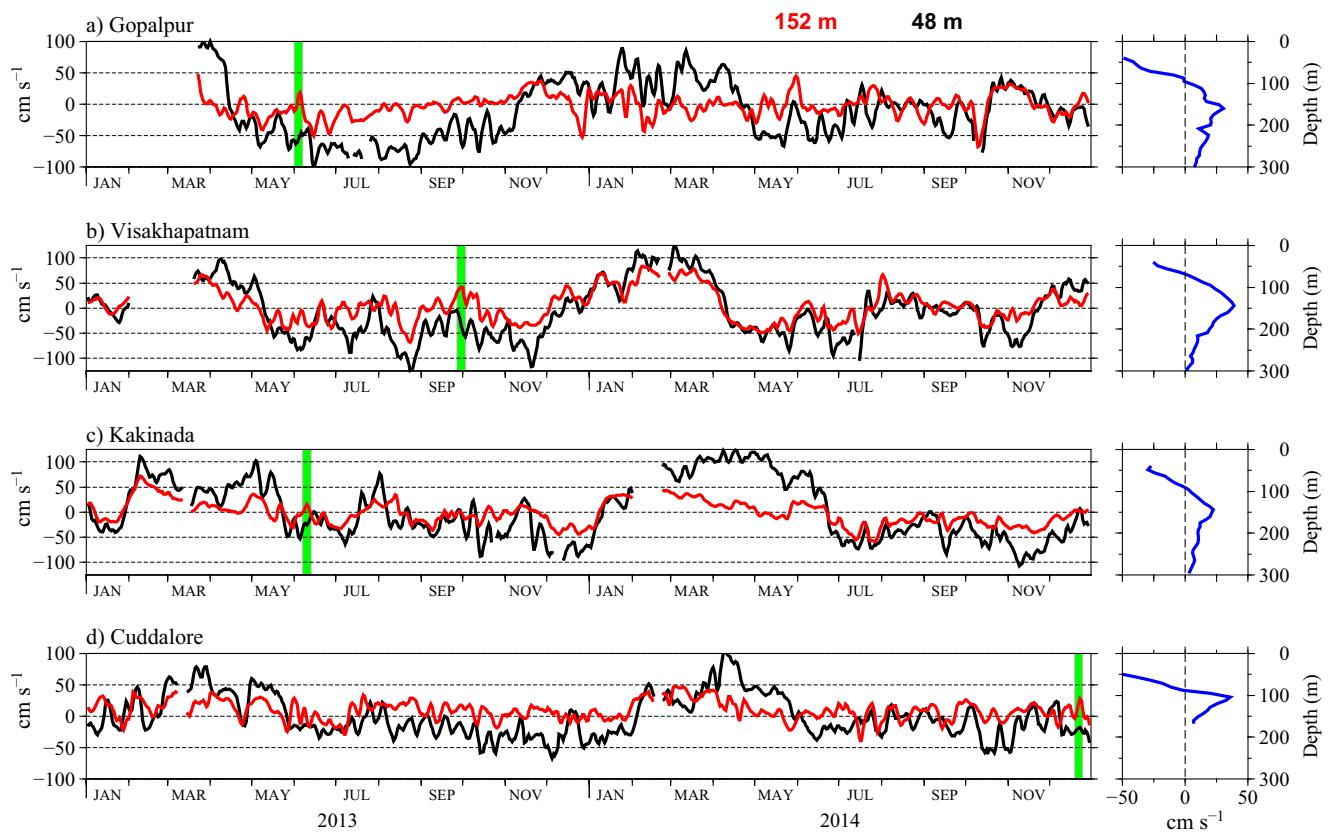
Fig. 2 Time series of observed alongshore component of current at 48 m (black) and 152 m (red) at different locations on the slope. Snapshot of vertical profiles of alongshore current when the undercurrents were observed is shown in the right panel. Green shades indicate the time which is used to plot vertical profiles in the right panel

(2014) for more information on the observed variability in the near-surface EICC.

Figure 2 shows that the alongshore currents at 152 m depth were relatively strong (70–90 cm s^{-1}), and they mostly followed the direction of the near-surface currents at all the locations during spring. This suggests that EICC extended to deeper levels during this season. In the rest of time (summer and winter), the subsurface flow direction often became opposite to that of the surface flow. Snapshots of vertical structure of alongshore currents (right panels in Fig. 2) on the slope show that the opposite flow mostly occurred below 75 m at all locations. To obtain a more integrated view of the vertical structure of the undercurrents, time-depth section of the observed alongshore currents at the ADCP locations is shown in Fig. 3. An interesting feature in EICC was the presence of poleward subsurface flow, which was opposite to the direction of the near-surface flow. This subsurface flow (undercurrents) extended even up to 700 m depth. The undercurrents were present at all the locations, but they occurred more frequently off Cuddalore. While the undercurrents were seen even at depths as shallow as 75 m in the observations from off Cuddalore (Fig. 3g), the undercurrents in the northern part of the coast (such as off Gopalpur and off Visakhapatnam) occurred at relatively deeper levels (100–150 m and more,

Fig. 3). Observed near-surface currents were equatorward on the slope off Cuddalore during summer and winter, but they were poleward during spring. The undercurrents were predominantly poleward during summer and winter. Significant variability in the intensity/direction in period of 10–20 day period was also observed during these seasons. It may be noted that the surface currents were not necessarily equatorward when the undercurrents occurred. For instance, episodes of equatorward undercurrents under the poleward surface flow occurred during late spring (April–May) off Kakinada and Cuddalore in 2014 (Figs. 2e and g).

The ADCP observations off Visakhapatnam and Gopalpur show that the occurrences of poleward undercurrents on the slope were less frequent compared to that of Cuddalore (Fig. 3a and c). The presence of undercurrents was limited, though not completely absent, in the observations from the slope off Kakinada (Fig. 3e). Signals of undercurrents can be seen in the observations on the slopes off Gopalpur, Kakinada, and Cuddalore in other years also (Fig. 2 in Mukherjee et al. 2014). One limitation of the ADCP observations from the continental slopes is the absence of data in the top 40 m of the water column. By analyzing the data on subsurface circulation from ADCP in conjunction with the data on surface flow from HF (high-frequency) radar, Mukhopadhyay et al.
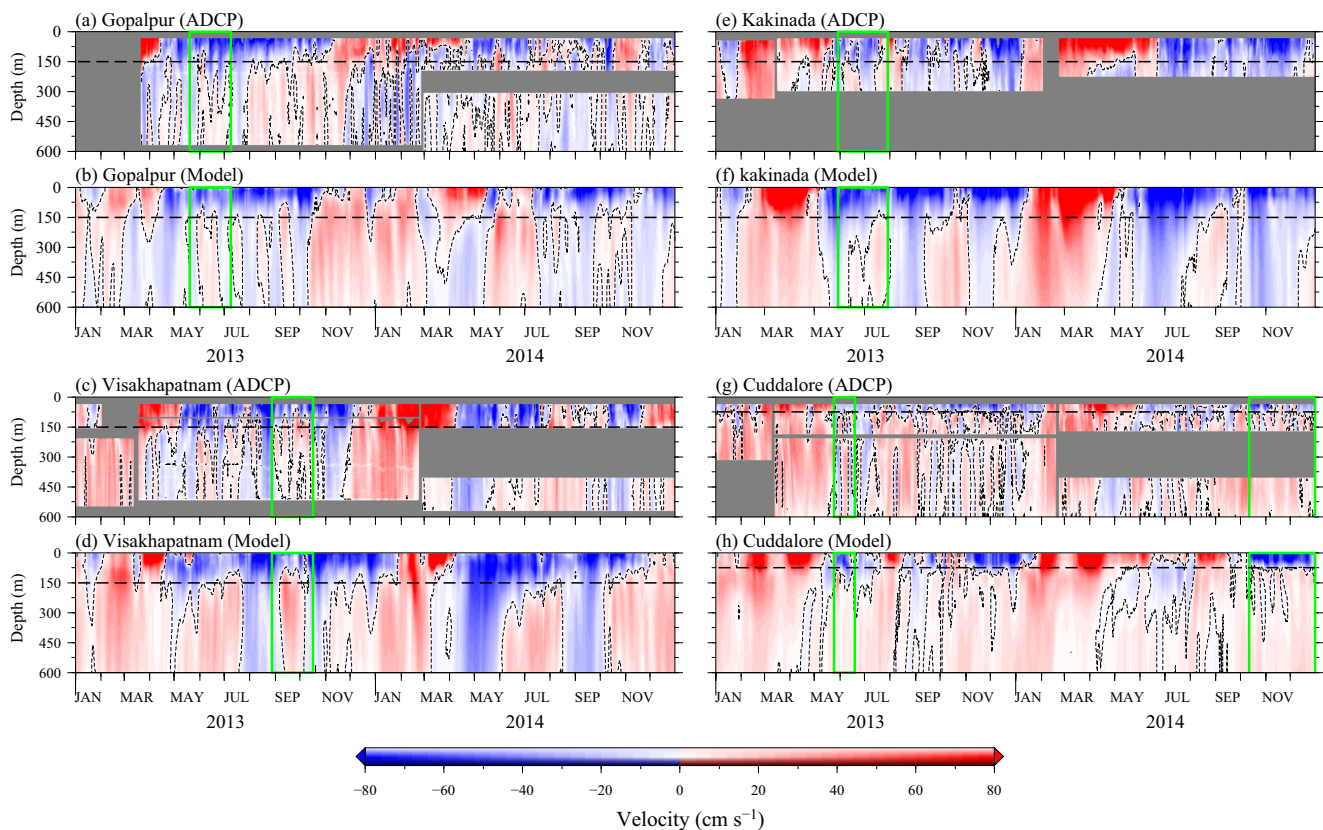
Fig. 3 Time-depth section of observed (ADCP) and modeled alongshore currents on the slope off Gopalpur (**a–b**), Visakhapatnam (**c–d**), Kakinada (**e–f**), and Cuddalore (**g–h**). Dashed line contours represent the zero values. Positive values indicate the poleward flow. Gray-shaded areas indicate data missing. Horizontal dashed lines indicate the approximate depth of undercurrent. Rectangular green boxes indicate the periods when model simulated the undercurrent feature very well and some of these events were used to examine the undercurrents features in detail

(2017) showed that while the surface flow during February/ March could be quite deep, during the summer and winter, it could be as shallow as 40 m, except in the northern part of the east coast. They also noted significant variability in the depths of the flow in the intraseasonal time scales (periods of the order of 20–45 days) comprising episodes having surface flow deepening up to 100 m depth.

3.2 Simulation of EICC by high-resolution model

Alongshore currents at the four locations discussed above, viz., Gopalpur, Visakhapatnam, Kakinada, and Cuddalore, derived from the model simulations, are shown along with the observations from the ADCPs in Fig. 3. The model was able to simulate many observed features of the surface as well as subsurface currents including the seasonal and intraseasonal variability in the magnitude and direction of currents, occurrences of poleward undercurrents, and the latitudinal variation in the depth of undercurrents realistically. Statistical validations, such as correlation, root mean square error (RMSE), and standard deviation of modeled alongshore currents with respect to the ADCP observations over the entire depth at all the ADCP locations considered in this study, are presented in Fig. 4. Values of correlation

coefficients of alongshore currents in the upper 100 m are in the range of about 0.5–0.7, which suggests that the model was able to simulate the observed variability of EICC in the upper ocean realistically. In the subsurface layers, i.e., 100–200 m, the values of the correlation are about 0.3–0.5. At all the locations, the correlation between the observations and the simulations is higher for the alongshore component of the currents compared to the cross-shore component. RMSE of alongshore currents at 48 m is in the range of 40–60 cm s^{-1} and the RMSE reduces considerably with depth. Very shallow surface flow during summer or fall/early winter described by Mukhopadhyay et al. (2017) is not seen in the model simulations for the period we considered in this study.

Since the specific attention of this paper is to address the undercurrents in the EICC, the performance of the model in simulating the subsurface coastal circulation at different time scales is quantified using wavelet coherence analysis between ADCPs and model at 152 m (Fig. 5). At Gopalpur, variability in alongshore currents in the period shorter than 30 days was simulated with good accuracy except during spring (Fig. 5a). At Visakhapatnam and Kakinada, best performance of the model (coherence higher than 0.8) was restricted to seasonal time scale (period more than 90 days) and also at higher-
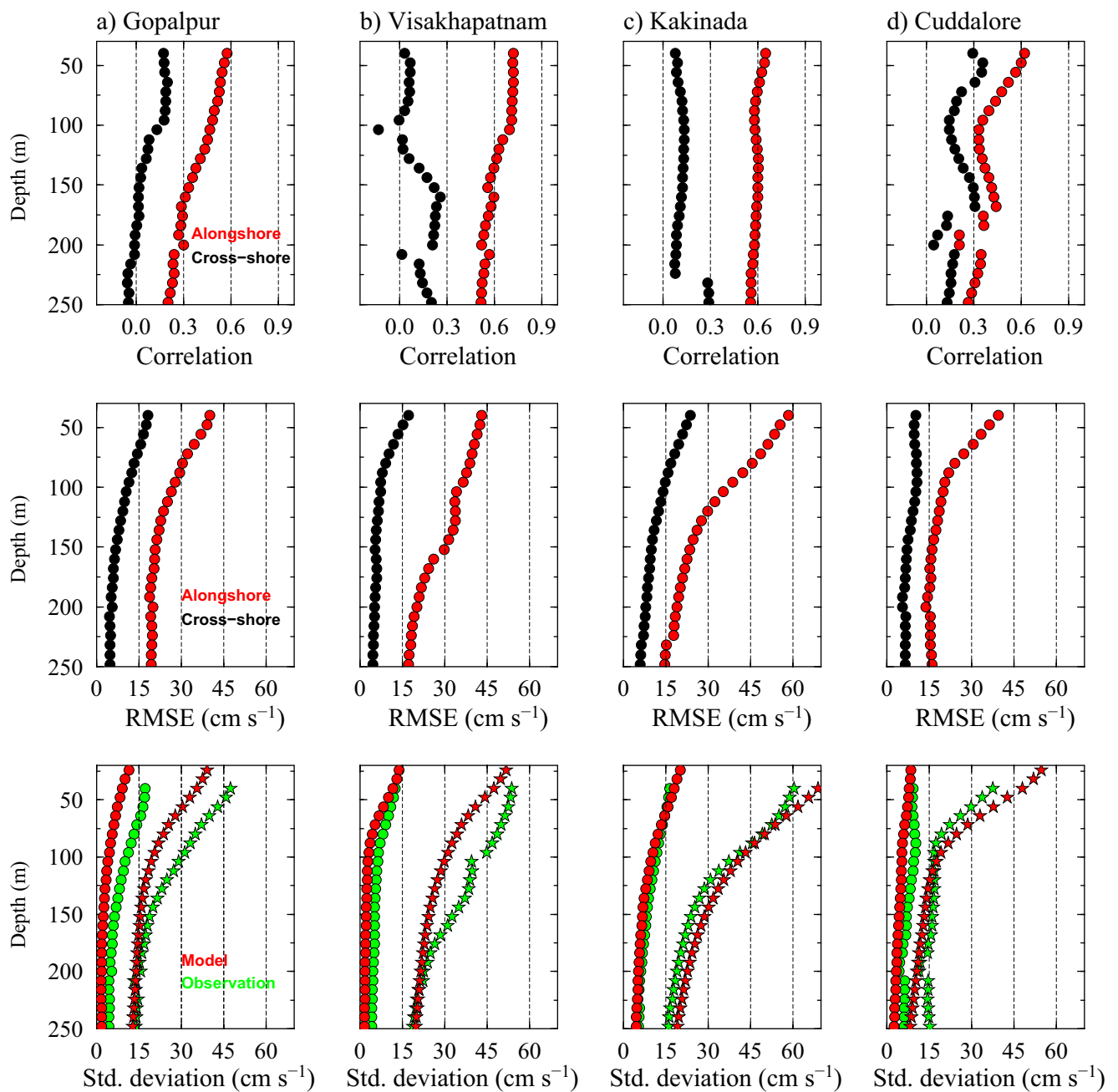
Fig. 4 Statistical comparison of modeled alongshore (star) and cross-shore (circles) current with ADCP observation at different locations on the slope during 2013–2014. Vertical profiles of correlation (upper panel), RMSE (middle panel), and standard deviation (third panel) are shown

frequency (period less than 30 days) intraseasonal time scale. However, a slight phase difference between the ADCP observations and the model simulations at seasonal periods (~180 days) was seen at both Kakinada and Visakhapatnam. At Visakhapatnam (Kakinada), 45° phase difference was observed in anticlockwise (clockwise) direction, which implies that the observation was leading (lagging) the model by about 20 days (Figs. 5b and c). At Cuddalore, the performance of the model was not very good at seasonal time scale compared to Kakinada. However, high coherence with almost no phase

difference between the observations and the model simulations at periods shorter than 30 days was observed at Cuddalore (Fig. 5d). In the intraseasonal band (30–90 days), significant coherence of alongshore currents can be noticed at Kakinada and Visakhapatnam. However, the coherence was not significant at Gopalpur and Cuddalore in the intraseasonal band.

As in the case of observations, the undercurrents were seen in the model simulations at all the locations considered, though they were quite prominent at Cuddalore compared to other locations, particularly during winter. Poleward currents
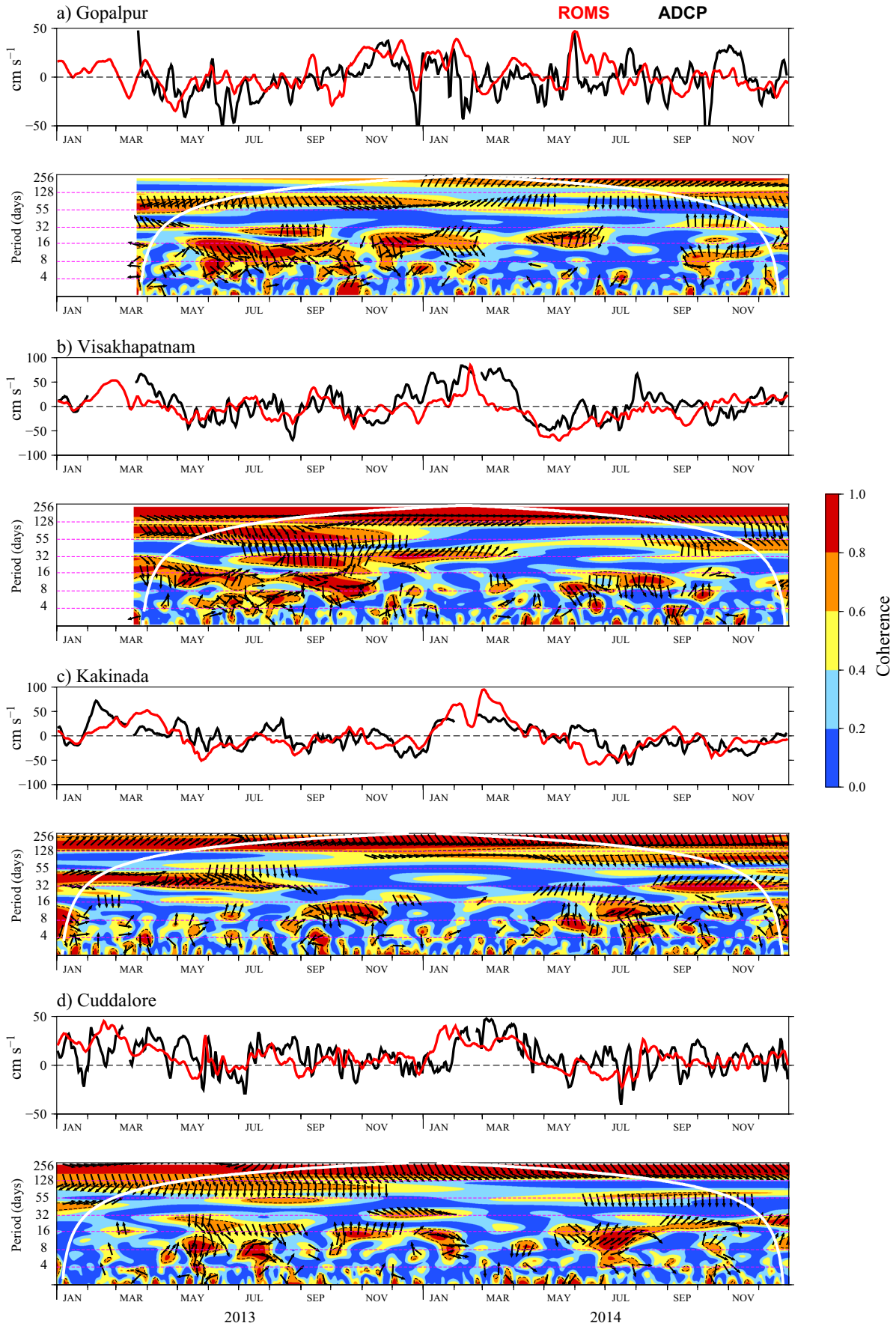
Fig. 5 Time series of observed and modeled alongshore current at 152 m on the slope off Gopalpur, Visakhapatnam, Kakinada, and Cuddalore. Wavelet coherence between ADCP and modeled alongshore currents at 152 m is also shown. The dashed contour line in the wavelet coherence spectra shows the 5% significance level against the red noise, and the thick white curve shows 95% significant COI (cone of influence). The vectors show the relative phase difference with in-phase (antiphase) pointing right (left). The first variable leads (lags) the second in the anticlockwise (clockwise) direction. The vectors are shown only for wavelet coherence of 0.5 or more

which extended into deeper layers at Cuddalore during January to April as well as the reversal of current direction (equatorward to poleward) occurred during October to March were also simulated well by the model. A realistic simulation of the surface and subsurface features of EICC at all the locations of ADCP gives us the confidence to rely upon these simulations to study the structure and dynamics of the undercurrents.

3.3 Structure and variability of model undercurrents along the western BoB

In the model simulations, direction of the EICC was mostly equatorward at Gopalpur and Visakhapatnam during both summer and winter seasons (Figs. 3b and d). Only during spring, the direction of the EICC was poleward at Gopalpur (Fig. 3b). Remotely forced signals propagating from the equatorial Indian Ocean primarily drives the equatorward flowing EICC during summer in the northern part of the coast (McCreary et al. 1996). The undercurrents on the slope off Visakhapatnam and Gopalpur were generally restricted below 150 m, and the equatorward surface currents at these locations were very close to the coast as a narrow stream (Fig. 3). Even though we noticed a few events with the presence of undercurrents at both locations, our analysis was restricted to the formation of undercurrents observed during September 2013 on the slope off Visakhapatnam (Fig. 3b and d), when the model simulated the undercurrent event more accurate. Observed sea level anomaly from AVISO (Archiving, Validation, and Interpretation of Satellite Oceanographic data, https://www.aviso.altimetry.fr/en/data.html) and modeled surface currents showed the presence of an anticyclonic eddy (in the surface as well as subsurface) centered around 87°E and 17°N during 20 August 2013 (Fig. 6). This anticyclonic eddy moved westward (toward the coast) and reached the continental slope off Visakhapatnam. The arrival of this eddy onto the slope weakened the magnitude of equatorward flowing EICC in the near-surface levels. Meanwhile, the strong circulation associated with this eddy (poleward flow at the western edge) reversed direction of equatorward flowing EICC into poleward in the subsurface levels (below 120 m). Hence, an equatorward surface flow and poleward subsurface flow were developed on the slope.

(Magenta boxes in Fig. 6). On 20 September 2013 (third panel in Fig. 6), the core of this undercurrent (40 cm s^{-1}) was observed at Visakhapatnam, and the extension of this undercurrents was evident on the slope off Gopalpur and even further north upto (20° N), both in the observations as well as the model simulations. This suggests that the poleward undercurrent observed in this region was the western edge of a well-defined westward propagating anticyclonic eddy seen in the offshore regions (Fig. 6).

A snapshot of modeled surface and subsurface currents off Cuddalore (for 15 November 2014) is shown in Fig. 7. The surface currents off Cuddalore were equatorward, and maximum magnitude was about 120–150 cm s^{-1}. This strong surface currents were associated with equatorward flowing EICC during winter, and its core was located just offshore of the ADCP mooring on the slope off Cuddalore. At the same time, below the equatorward surface flow (at about 150 m depth), an anticyclonic eddy with a horizontal extent of about 20–30 km (hereafter referred as small-scale eddy) was seen on the slope (indicated with magenta box in Fig. 7b). The poleward undercurrents observed at the ADCP location on the slope (below 75 m) were associated with this small-scale eddy, which was found to be well-developed around 200 m depth, and its strength gradually reduced in deeper layers. Below 500 m, this small-scale eddy was absent, and the poleward undercurrent at the ADCP location on the slope off Cuddalore was an extension of anticyclonic subsurface eddy with a diameter of about 200 km (hereafter referred as mesoscale eddy). This mesoscale eddy was clearly seen below 500 m, and core of this eddy was centered about 200 km away from the coast of Cuddalore (Figs. 7e and f). By about 1200 m depth, the major circulation pattern observed was this anticyclonic mesoscale eddy alone as other eddies present in the surface/subsurface disappeared/weakened (Figs. 7e and f).

We also examined the surface and subsurface currents off Cuddalore on 3 December 2014 to identify the variability and propagation of these mesoscale anticyclonic eddies (Fig. 8). It was found that small-scale eddy observed on the slope (100–200 m) was located at the same position even after 23 days, which indicates that this system was nearly stationary. Detailed discussion on the variability and formation of this small-scale eddy is given in Section 3.3. Longitude-depth section of the alongshore currents shown in Fig. 9 suggests that the core of the undercurrent at the latitude of Cuddalore (12°N) was about 100 km away (in cross-shore direction) from the coast and the speed of this alongshore current was maximum (about 35 cm s^{-1}) at a depth of 1200 m. However, as inferred from Fig. 7f and Fig. 8f, the location at which maximum speed (about 50 cm s^{-1}) of this undercurrent system (anticyclonic eddy) was slightly toward the northeast of the ADCP mooring location. The offshore anticyclonic eddy can be clearly seen in the sea level anomaly pattern given in Fig. 10. Even though a good correspondence between the
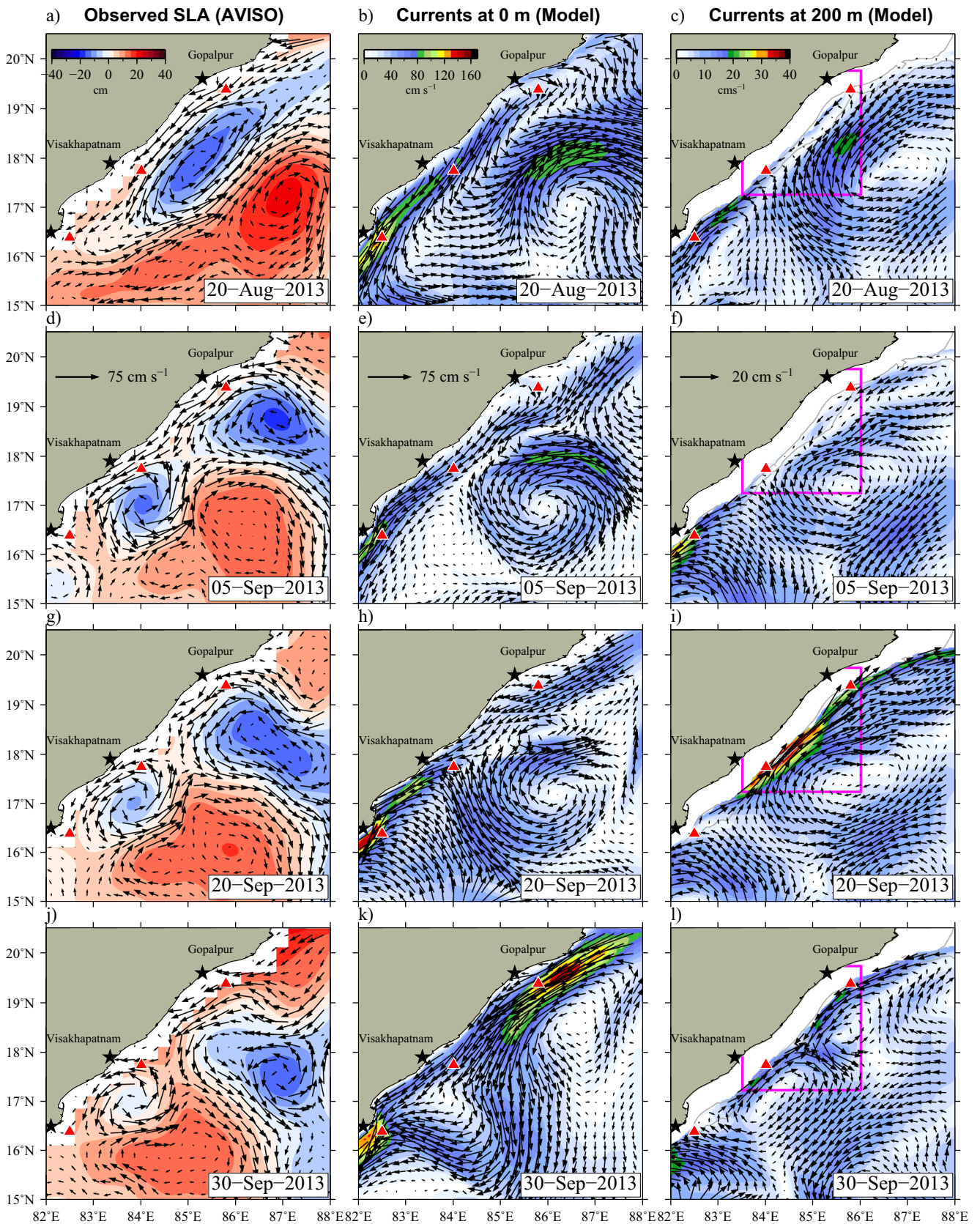
sea level anomaly and the surface circulation was observed (Fig. 10), core of the subsurface mesoscale anticyclonic eddy did not coincide with the high in the sea level anomaly (Fig. 8f). This was essentially due to the northwest tilt in the

axis of anticyclonic eddy with depth. Further, it may be seen from Fig. 10 that this eddy had strengthened and moved in the northwest direction in the subsequent days (25 November 2014). When this eddy reached near the continental slope off Cuddalore (5 December 2014), the surface EICC weakened significantly, and the poleward undercurrents further

strengthened with its magnitude exceeding 50 cm s^{-1} at 1200 m depth (Fig. 8f). It may be noted that westward propagating anticyclonic eddies in the southern part of the BoB during late fall/early winter were reported in earlier studies also (Vinayachandran et al. 2005).

In short, the undercurrents seen below the EICC, both in the northern part as well as the southern part of the coast, were not continuous poleward flows but were part of distinct anticyclonic eddies. These anticyclonic circulations were either downward extensions of the surface eddies (off Gopalpur and Visakhapatnam) or they were very localized small-scale anticyclonic circulation limited to about 250 m depth (off Cuddalore). During most of the events, the net effect of strong equatorward EICC and relatively weak poleward component of flow in the western part of the anticyclonic eddy were seen as equatorward
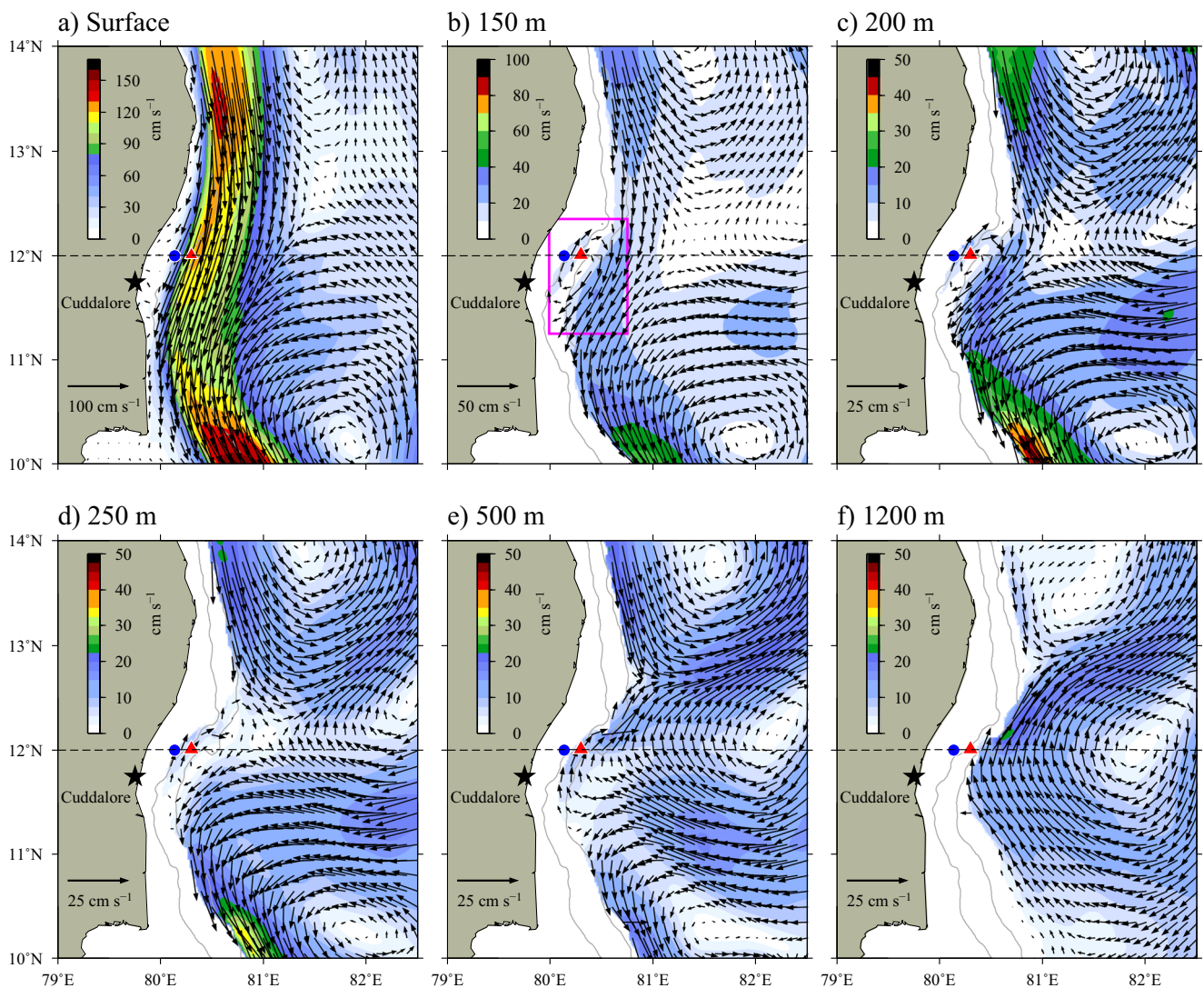

Fig. 7 Circulation pattern off Cuddalore at different depths on 15 November 2014. Vectors show the current direction, and overlaid is the current magnitude (cm s^{-1}). Note that the scales of current vectors and color bar are different at each subplot. Blue circle (red triangle) represents the location of ADCP deployed on the shelf (slope). Dashed black line represents the 12°N latitude. Continuous gray lines represent the 100 m and 1000 m bathymetric contours. Rectangular box (magenta) indicates the subsurface eddy near the shelf break
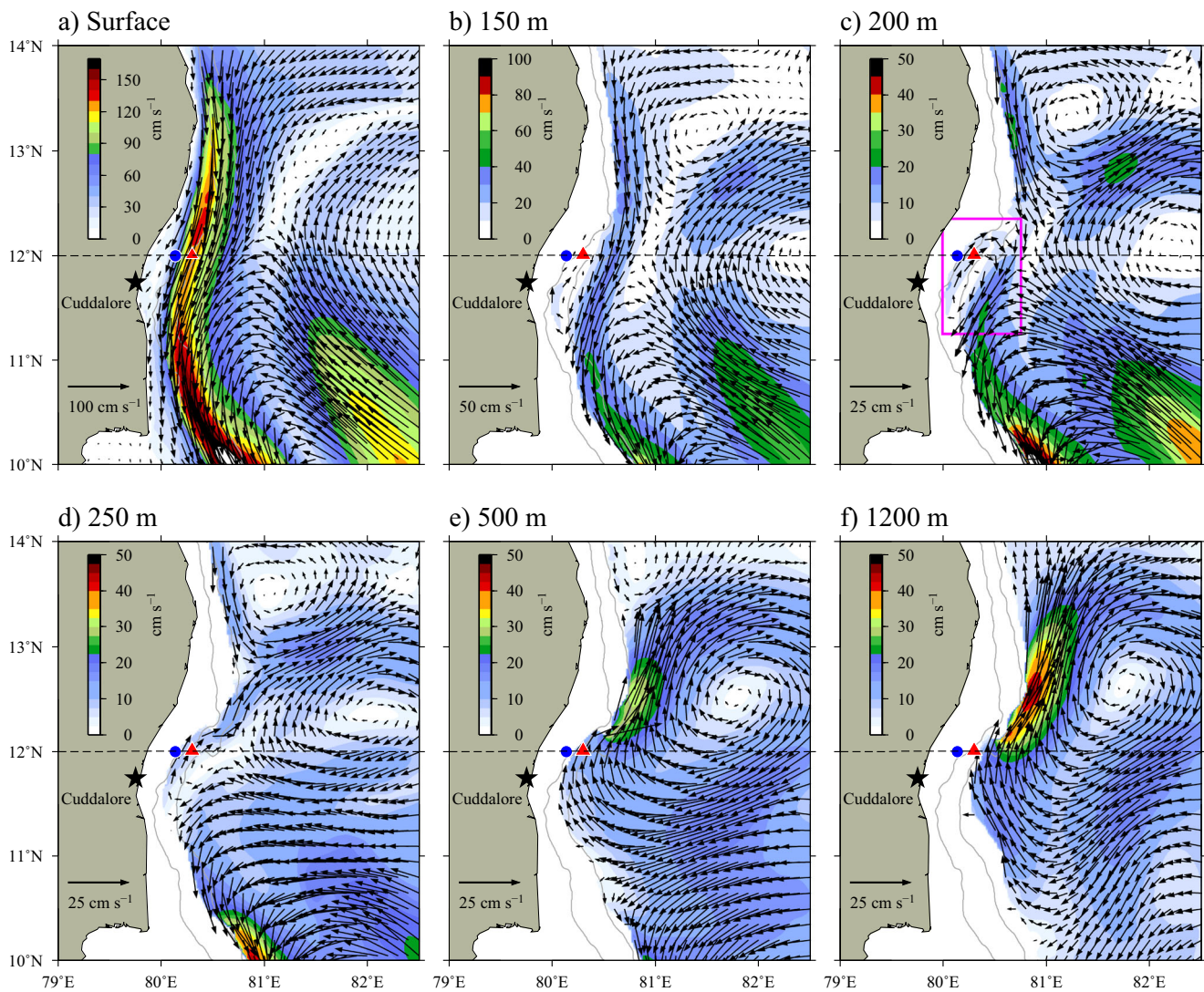
Fig. 8 Same as Fig. 3 but for on 3 December 2014

flow near the surface. As the strength of EICC waned with depth, the poleward flow became the dominant one, generating a coastal undercurrent. In the next section, we examine how very localized, distinct, small-scale mesoscale anticyclonic systems, which were not part of the mesoscale anticyclonic systems in the deep ocean, were formed near the shelf break off Cuddalore.

3.4 Dynamics of the formation of small-scale anticyclonic eddies off the coast of Cuddalore

As discussed earlier, an important feature of the subsurface circulation off Cuddalore was the presence of strong undercurrents seen in winter at deeper levels (∼ 1200 m) as part of large-scale anticyclonic circulations (Figs. 7 and 8). However, in late spring (May–June 2013) and winter (2013 and 2014), the presence of distinct small-scale anticyclonic circulations at a depth of about 100 m to 200 m was responsible for the poleward undercurrents observed at

the ADCP location. The size of these eddies were about 20–30 km in diameter, and their signatures were not seen in the surface. Identifying the reasons for the formation and evolution of these small-scale eddies is hence important for understanding the variability in the observed undercurrents in this region. Figure 11 shows the time series of observed and modeled alongshore currents off Cuddalore during autumn and early winter. Observations show that the magnitude of undercurrent on the shelf was about 20–30 cm s^{-1}, and it was relatively stronger on the slope with magnitude of about 30–40 cm s^{-1} (Fig. 11a and b). The observed signature of the undercurrent was more distinct on the slope, whereas its signal was weak on the shelf. On the slope, the magnitude of undercurrents exhibited a higher intraseasonal variability around 100–200 m. Below 300 m, the undercurrent was relatively steady (Fig. 11b). Model simulations also show similar features of the undercurrent on the slope, though the magnitude of modeled
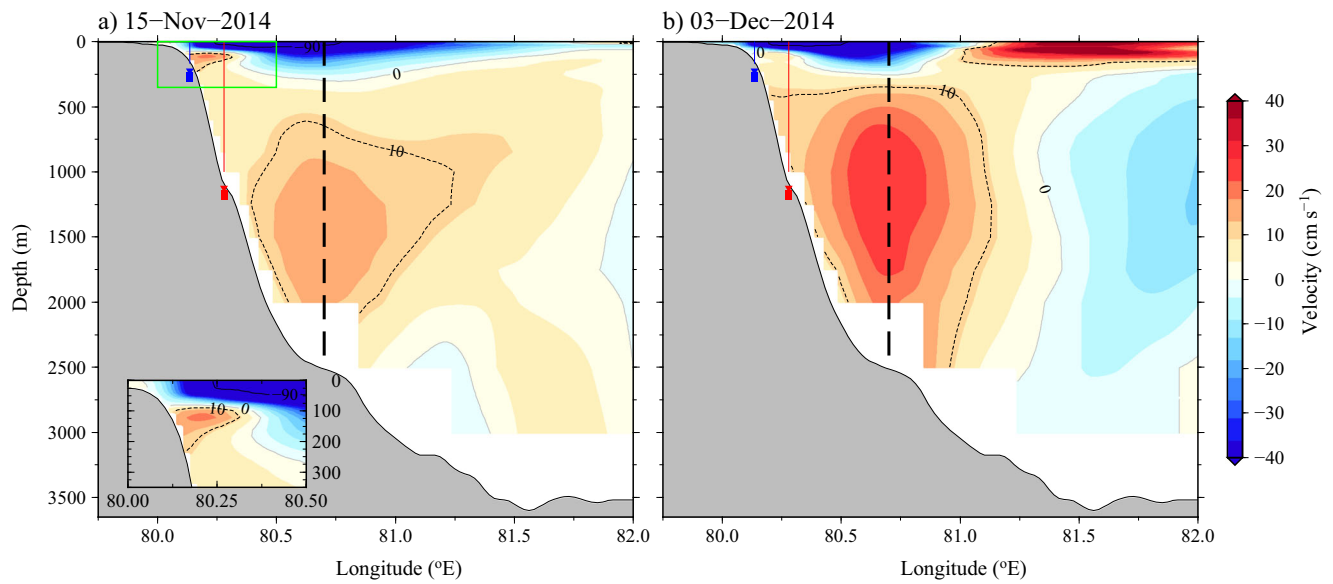
Fig. 9 Longitude-depth section of alongshore currents at 12°N on (a) 15 November 2014 and (b) 3 December 2014. Positive values indicate the poleward flow. Inset plot is the zoomed view of shelf break region indicated by green box. Dashed black vertical line shows the core of the undercurrent, and red (blue) vertical lines shows the location of ADCP observation on the slope (shelf)

undercurrent was weaker than the observation (Fig. 11c). This difference in the strength of intraseasonal variability indicates that the poleward undercurrent seen at a depth of 100–200 m and those seen in the deeper levels could be independent. Further, in general, it was also observed (Fig. 11c) that the poleward undercurrents at a depth of 100–200 m strengthened with the intensification of the equatorward EICC in the surface layers (with a slight delay on some events). This clearly suggests that the variability in the strength of surface EICC played a critical role in the observed variability in the strength of the undercurrents near the shelf break.

Figure 1b shows that the coastline as well as the 100 m isobath near Cuddalore has a concave-shaped curvature (inward). In addition, the width of the continental shelf north of Cuddalore (12.5°N) is much broader than the shelf near Cuddalore (Fig. 1b). Due to these bathymetric features, the core of the EICC shifted about 40–50 km away from the ADCP location on the slope off Cuddalore and hence setup a zonal gradient of velocity in the alongshore current between the coast and core of the EICC (Fig. 9). This zonal (east-west) gradient of velocity in the EICC was very strong near the shelf break. The strong gradient of velocity in the alongshore currents setup negative relative vorticity ($\frac{dv}{dx} - \frac{du}{dy}$) in this region, and a clockwise circulation was developed between the core of the EICC and the shelf break (Fig. 11d). Since the zonal variation of the meridional component ($\frac{dv}{dx}$) of EICC was the strongest term in the relative vorticity expression ($\frac{du}{dy}$ was less

than 10% of $\frac{dv}{dx}$), only this term was considered in the present analysis (Fig. 11d). Depending on the intensity of the velocity gradient ($\frac{dv}{dx}$), which was directly linked to the intensity of the surface flow itself, these clockwise circulations further developed as anticyclonic subsurface eddies.

The momentum budget (Fig. 11e) estimated for the model simulated subsurface currents (200 m) on the shelf break (80.25°E, red vertical line in Fig. 11f) shows that their alongshore and cross-shore components were almost in geostrophic balance (balance between pressure gradient force and Coriolis force). This reconfirms that the poleward undercurrents seen below the shelf break (> 250 m) were part of this subsurface anticyclonic eddies, which were in quasi-geostrophic balance. Since the formation/evolution of these anticyclonic eddies was linked to the intensity of the surface flow, the strength of the undercurrents was also seen to be linked to the strength of the surface flow (Fig. 11c). In other words, the negative relative vorticity near the shelf break increased with the intensification of the surface EICC, which resulted in the strengthening of the undercurrents. This variation in the strength of undercurrents was seen as their fluctuations in the intraseasonal or even in shorter time scales (10–20 day). As mentioned earlier (Section 1), intraseasonal variability in the surface currents is linked to many factors including the intensity of alongshore winds along the east coast of India, wind stress in the interior BoB, as well as the remote forcing from the equatorial Indian Ocean. Therefore, these factors are also expected to cause intraseasonal variability in the undercurrents.
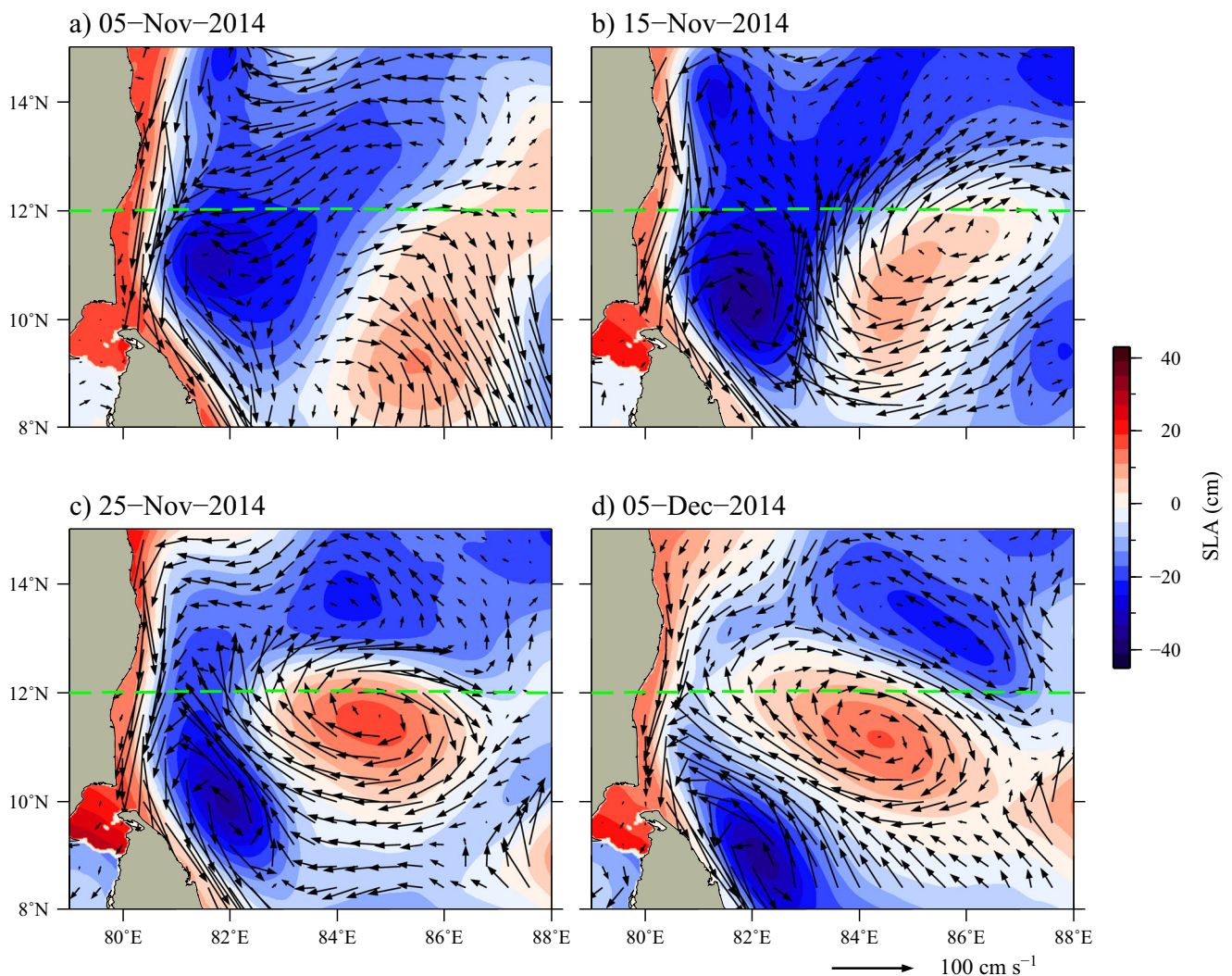
Fig. 10 Evolution of modeled sea level anomaly and surface currents off Cuddalore. Direction of surface current is plotted as vectors over sea level anomaly. Dashed green line represents 12°N latitude

Note that ADCP observations from the shelf showed only a weak signal of undercurrents, whereas they were more prominent in the data from the ADCPs deployed on the continental slope. Figure 11g shows that the ADCP mooring on the shelf is located in the onshore edge of the undercurrents (indicated with magenta line in Figs. 11g) generated on the shelf break and ADCP mooring on the slope is located at the core of the undercurrents. This explains why more prominent signals of undercurrent were seen on the slope. In addition, this also suggests that undercurrents were mostly concentrated on slope and shelf break and not extending into the inner shelf.

We further examined the formation of undercurrent system observed during late spring/early summer (May–June) 2013 to ascertain whether the same

mechanism was responsible for this event also (Fig. 12). Equatorward surface currents seen off Cuddalore in late spring/early summer in 2013 were found to be associated with the anticyclonic eddy in the southwestern BoB (Fig. 12d). However, unlike the poleward undercurrents observed during winter, these currents in late spring/early summer were limited very close to the shelf break and relatively shallow. Core of these undercurrents (up to 25 cm s^{-1}) was seen between 100 and 200 m. Below 200 m, the undercurrents were weak (less than 10 cm s^{-1}). These poleward undercurrents were again due to a small-scale anticyclonic eddy formed on the shelf break (Fig. 12e). However, formation of this anticyclonic eddy near the shelf break was associated with the westward propagating mesoscale cyclonic eddy in the surface. When this cyclonic eddy
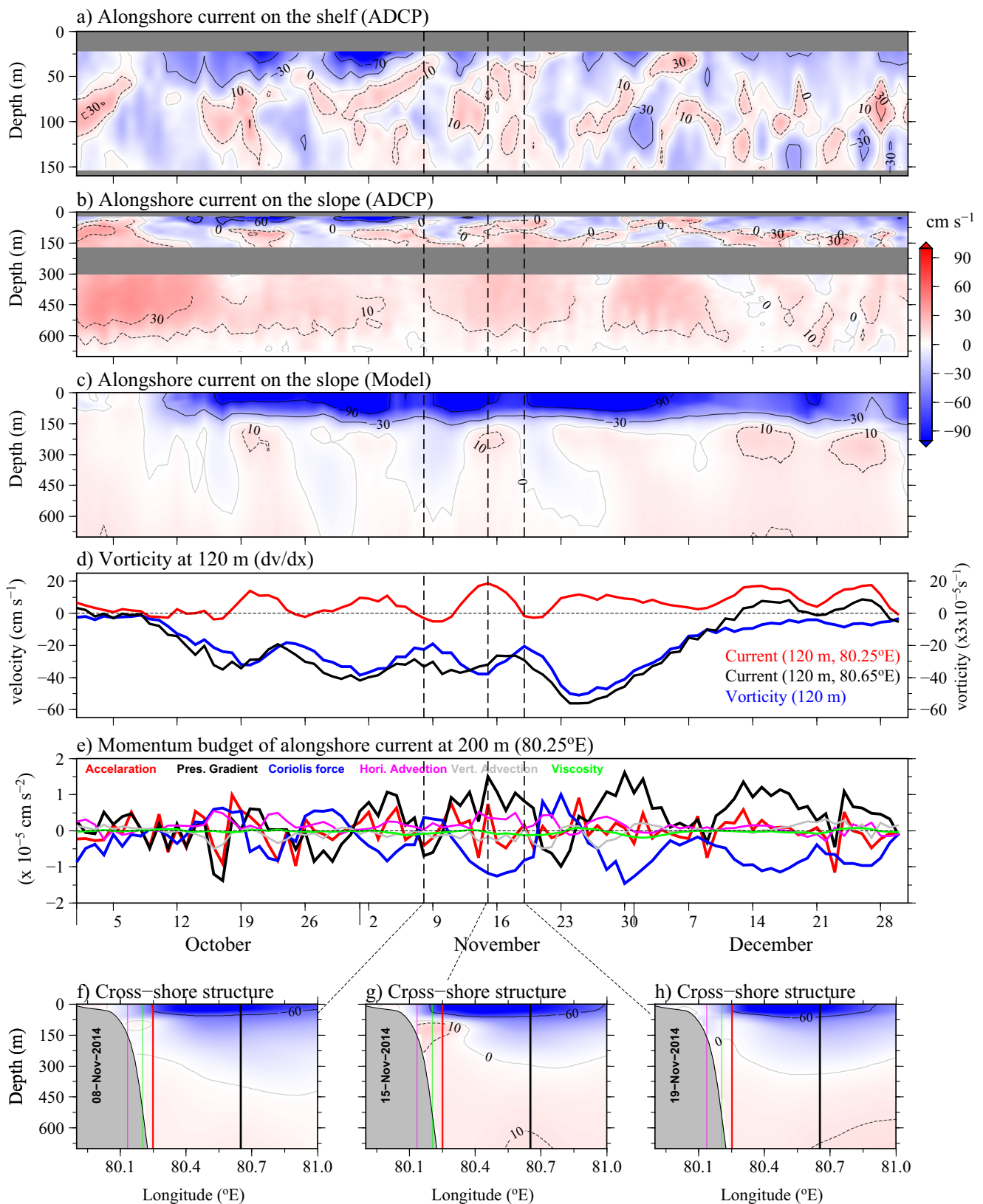
Fig. 11 Time-depth section of observed daily-mean alongshore currents (cm s^{-1}) on the shelf (**a**) and slope (**b**) off Cuddalore for the period 1 October 2014 to 31 December 2014. (**c**) Time-depth section of the daily-averaged alongshore current on the slope off Cuddalore (80.3°E, 12°N). (**d**) Time series subsurface alongshore current (120 m) at 80.25°E (red line) and 80.65°E (black). Relative vorticity (blue) at 120 m (dv/dx) is calculated between 80.25°E and 80.65°E. (**e**) Momentum budget terms for the alongshore component of undercurrents at 200 m on the slope (80.25°E). (**f–h**) Cross-shore structure of alongshore current at 12°N. Red and black vertical lines indicate the 80.25°E and 80.65°E longitudes used to calculate relative vorticity, respectively. Magenta (green) vertical lines indicate longitudes of the locations of ADCP mooring on the shelf (slope)
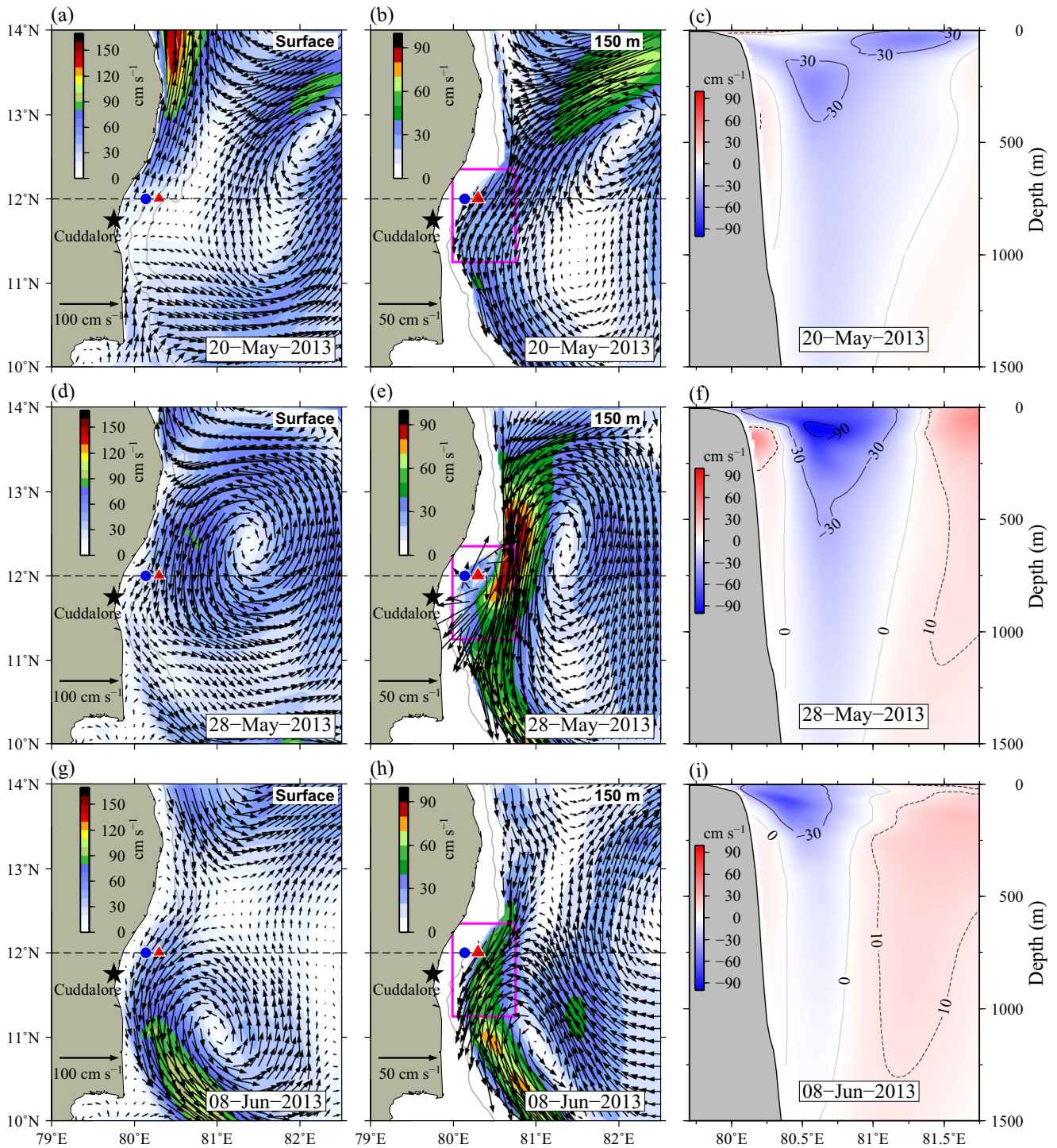
Fig. 12 Evolution of surface circulation pattern and associated change in the undercurrents off Cuddalore. First column (a, d, and g) shows the southwest propagation of cyclonic eddy. Vector shows the current direction, and overlaid is the magnitude (cm s^{-1}). Second column (b, e, and h) shows the intensification of undercurrents associated with the propagation of eddy. Rectangular box (magenta) indicates the region where the subsurface eddy formed near the shelf break. Third column (c, f, and i) shows the associated change in the alongshore currents in the cross-shore direction

approached the continental slope, the zonal shear in the alongshore currents increased (due to the concave shape of bathymetry), which eventually resulted in the formation of anticyclonic circulation near the shelf break (Fig. 11). This was seen as the undercurrents in the ADCP observation.

4 Summary and discussions

In this paper, we described the structure and formation of undercurrents off the east coast of India (western BoB) by analyzing the ADCP observations and the simulations from a very high-resolution ocean general circulation model for the period January 2013 to December 2014. In the northern ADCP locations such as Gopalpur and Visakhapatnam, poleward undercurrents observed on the slope at depth below 150 m were subsurface signatures of the westward propagating anticyclonic eddies. When these anticyclonic eddies approached the coast, the poleward flowing currents associated with anticyclonic eddy overcame the southward flow in the subsurface (below 150 m), resulting in poleward undercurrents.

Observations show that the undercurrents in the southern part of the east coast (off Cuddalore) were more prominent and persisted for a longer period, especially during October to December. We show that the observed poleward undercurrents below the equatorward EICC in this region were associated with two different subsurface anticyclonic circulations: one formed near the shelf break (100–200 m) and another in the deep region (below 500 m). It has been further shown that the observed high-frequency fluctuations in the coastal undercurrents on the shelf break at a depth of ~ 100–200 m off the coast of Cuddalore were associated with local generation of subsurface anticyclonic eddies with a diameter of 20–30 km, which were generated due to strong zonal shear in the EICC below the shelf break. Since the zonal shear in the EICC near the shelf break was essentially linked to the strength of the flow itself, the formation of undercurrents and their short period (10–20 day) variability in the strength was closely related to the variability of the EICC. The second system found in the deep ocean region (> 500 m depth) was part of a large persistent subsurface anticyclonic eddy. Model simulations suggest that this system moved northwestward and induced strong undercurrents (about 50 cm s^{-1} at 1200 m depth) as it interacted with the continental slope off Cuddalore. In the southern part of the western BoB (off Cuddalore), undercurrents were mainly observed at about 75 m depth, whereas they were about 150 m depth on the northern part of the western BoB (Off Visakhapatnam and Gopalpur). Shallow

undercurrents seen in the southern part of the coast were associated with the formation of anticyclonic eddy close to the shelf break.

There have been several studies on the presence of mesoscale eddies in the undercurrent systems in the global oceans. For example, Qu et al. (2012) showed the presence of mesoscale eddies in the Mindanao Undercurrent (MUC) system in the western Pacific, which are generated from strong instability arising from the shear in mean flow. They showed that these mesoscale eddies in the MUC transport freshwater northward beyond the limits of the mean flow along the offshore edge of the Philippine coast from South Pacific. Qiu et al. (2015) also showed that eddies in the MUC are generated by the baroclinic instabilities in the overlying western boundary currents. Thomsen et al. (2016) showed that one of the direct implications of the formation of such a subsurface anticyclone in the Peru-Chilean undercurrents is the ventilation of otherwise oxygen-deficient subsurface waters. They further showed that since the anticyclonic eddies in the Peru-Chilean current grow rapidly by drawing energy from the instability in the flow and move away, these eddies carry nutrients and biogeochemical tracers from coastal waters to open ocean.

Since many rivers discharge into the BoB, it is possible that the freshwater and physical and biogeochemical tracers associated with this discharge get transported alongshore/cross-shore by the subsurface eddies as in the case of many other undercurrent systems in the global oceans. However, such transports associated with subsurface eddies have not been addressed so far in the EICC region. The results from this paper, which presents the evidences of mesoscale and small-scale eddies in the undercurrents, suggest the necessity of such studies using observations and coupled biophysical models.

References

Akhil VP, Durand F, Lengaigne M, Vialard J, Keerthi MG, Gopalakrishna VV, Deltel C, Papa F, de Boyer MC (2014) A modeling study of the processes of surface salinity seasonal cycle in the bay of Bengal. J Geophys Res Oceans 119(6):3926–3947

Amol P, Shankar D, Fernando V, Mukherjee A, Aparna S, Fernandes R, Michael G, Khalap S, Satelkar N, Agarvadekar Y, Gaonkar M, Tari A, Kankonkar A, Vernekar S (2014) Observed intraseasonal and seasonal variability of the West India coastal current on the continental slope. J Earth Syst Sci 123:1045–1074

Chatterjee A, Shankar D, McCreary JP, Vinayachandran PN, Mukherjee A (2017) Dynamics of Andaman Sea circulation and its role in connecting the equatorial Indian Ocean to the Bay of Bengal. J Geophys Res 122:3200–3218

Fairall CW, Bradley EF, Rogers DP, Edson JB, Young GS (1996) Bulk parameterization of air–sea fluxes for TOGA COARE. J Geophys Res 101:3747–3764

Haidvogel DB, Beckmann A (1999) Numerical Ocean circulation modeling. Imperial College Press London 318

Haidvogel DB, Arango HG, Hedstrom K, Beckmann A, Malanotte-Rizzoli P, Shchepetkin AF (2000) Model evaluation experiments in the North Atlantic Basin: simulations in nonlinear terrain-following coordinates. Dyn Atmos Oceans 32:239–281

Han W, McCreary JP (2001) Modeling salinity distributions in the Indian Ocean. J Geophys Res Oceans 106(C1):859–877

Jensen TG (1991) modeling the seasonal undercurrents in the Somali current system. J Geophys Res 96:22151–22167

Jensen TG (2001) Arabian Sea and bay of Bengal exchange of salt and tracers in an ocean model. Geophys Res Lett 28(20):3967–3970

Jithin AK, Francis PA, Chatterjee A, Suprit K, Fernando V (2017) Validation of the simulations by the high-resolution operational ocean forecast and reanalysis system (HOOFS) for the Bay of Bengal. Tech rep ESSO/INCOIS/ ISG/TR/01(2017) http://moeseprints.incois.gov.in/4418/

Jithin AK, Francis PA, Unnikrishnan AS, Ramakrishna SVSS (2019) Modeling of internal tides in the western Bay of Bengal : characteristics and energetics. J Geophy Res Oceans 124:1–27. https://doi.org/10.1029/2019JC015319

Large WG, McWilliams JC, Doney SC (1994) Oceanic vertical mixing: a review and a model with a nonlocal boundary layer parameterization. Rev Geophys 32:363–403

Leetmaa A, Quadfasel DR, Wilson D (1982) Development of the flow field during the onset of the Somali current, 1979. J Phys Oceanogr 12:1325–1342

McCreary JP, Kundu PK, Molinari RL (1993) A numerical investigation of dynamics, thermodynamics and mixed-layer processes in the Indian Ocean. Prog Oceanogr 31:181–244

McCreary JP, Han W, Shankar D, Shetye SR (1996) Dynamics of the East India coastal current, 2, numerical solutions. J Geophys Res 101: 13993–14010

Mukherjee A, Kalita BK (2019) Signature of La Niña in interannual variations of the East India coastal current during spring. Cli Dynam 53:551–568

Mukherjee A, Shankar D, Fernando V, Amol P, Aparna S, Fernandes R, Michael G, Khalap S, Satelkar N, Agarvadekar Y, Gaonkar M, Tari A, Kankonkar A, Vernekar S (2014) Observed seasonal and intraseasonal variability of the East India coastal current on the continental slope. J Earth Syst Sci 123:1197–1232

Mukherjee A, Shankar D, Chatterjee A, Vinayachandran PN (2017) Numerical simulation of the observed near-surface East India coastal current on the continental slope. Cli Dynam 50:3949–3980

Mukhopadhyay S, Shankar D, Aparna SG, Mukherjee A (2017) Observations of the sub-inertial, near-surface East India coastal current. Cont Shelf Res 148:159–177

Naqvi SW, Narvekar PV, Desa E (2006) Coastal biogeo-chemical processes in the North Indian Ocean. The Sea 14:723–780

Qiu B, Chen S, Rudnick DL, Kashino Y (2015) A new paradigm for the North Pacific subthermocline low-latitude western boundary current system. J Phys Oceanogr 45(9):2407–2423

Qu T, Chiang TL, Wu CR, Dutrieux P, Hu D (2012) Mindanao current/undercurrent in an eddy-resolving GCM. J Geophys Res Oceans 117:C6026

Quadfasel DR, Schott F (1983) Southward sub-surface flow below the Somali current. J Geophys Res Oceans 88:5973–5979

Saji NH, Goswami BN, Vinayachandran PN, Yamagata T (1999) A dipole mode in the tropical Indian Ocean. Nature 401:360–363

Shankar D, McCreary JP, Han W, Shetye SR (1996) Dynamics of the East India coastal current 1. Analytic solutions forced by interior Ekman pumping and local alongshore winds. J Geophys Res 101:13975–13991

Shankar D, Vinayachandran PN, Unnikrishnan AS (2002) The monsoon currents in the North Indian Ocean. Prog Oceanogr 52:63–120

Shchepetkin AF, McWilliams JC (2005) The regional ocean modeling system (ROMS): a split-explicit, free-surface, topography-following-coordinate oceanic model. Ocean Model 9(4):347–404

Shenoi SSC, Shankar D, Shetye SR (2002) Differences in heat budgets of the near-surface Arabian Sea and Bay of Bengal: Implications for the summer monsoon. J Geophys Res 107:1–14

Sherin VR, Durand F, Gopalkrishna VV, Anuvinda S, Chaitanya AV, Bourdallé-Badie R, Papa F (2018) Signature of Indian Ocean dipole on the western boundary current of the bay of Bengal. Deep Sea Res I Oceanogr Res Pap 136:91–106

Shetye S, Shenoi S, Gouveia A, Michael G, Sundar D, Nampoothiri G (1991) Wind driven coastal upwelling along the western boundary of the Bay of Bengal during the southwest monsoon. Cont Shelf Res 11:1397–1408

Shetye SR, Gouveia AD, Shenoi SSC, Sundar D, Michael GS, Nampoothiri G (1993) The western boundary current of the seasonal subtropical gyre in the Bay of Bengal. J Geophys Res 98:945–954

Sindhu B, Suresh I, Unnikrishnan A, Bhatkar N, Neetu S, Michael G (2007) Improved bathymetric datasets for the shallow water regions in the Indian Ocean. J Earth Syst Sci 116:261–274

Song Y, Haidvogel DB (1994) A semi-implicit ocean circulation model using a generalized topography-following coordinate system. J Comput Phys 115:228–244

Thomsen S, Kanzow T, Krahmann G, Greatbatch RJ, Dengler M, Lavik G (2016) The formation of a sub-surface anticyclonic eddy in the Peru-Chile undercurrent and its impact on the near-coastal salinity, oxygen, and nutrient distributions. J Geophys Res Oceans 121(1):476–501

Vinayachandran PN, Shetye SR, Sengupta D, Gadgil S (1996) Forcing mechanisms of the bay of Bengal circulation. Curr Sci 71:753–763

Vinayachandran PN, Kagimoto T, Masumoto Y, Chauhan P, Nayak SR, Yamagata T (2005) Bifurcation of the East India coastal current east of Sri Lanka. Geophys Res Lett 32:15606–15606

Yu L, O'Brien JJ, Yang J (1991) On the remote forcing of the circulation in the bay of Bengal. J Geophys Res 96:20449–20454